

# RSC Sustainability

Accepted Manuscript

This article can be cited before page numbers have been issued, to do this please use: I. H. Nurwahid, S. K. Ismail, V. Natasya, J. Choi, K. Kim, S. Jin, H. Lee, C. Yoo, J. Ha and C. S. Kim, *RSC Sustainability*, 2026, DOI: 10.1039/D6SU00148C.



This is an Accepted Manuscript, which has been through the Royal Society of Chemistry peer review process and has been accepted for publication.

Accepted Manuscripts are published online shortly after acceptance, before technical editing, formatting and proof reading. Using this free service, authors can make their results available to the community, in citable form, before we publish the edited article. We will replace this Accepted Manuscript with the edited and formatted Advance Article as soon as it is available.

You can find more information about Accepted Manuscripts in the [Information for Authors](#).

Please note that technical editing may introduce minor changes to the text and/or graphics, which may alter content. The journal's standard [Terms & Conditions](#) and the [Ethical guidelines](#) still apply. In no event shall the Royal Society of Chemistry be held responsible for any errors or omissions in this Accepted Manuscript or any consequences arising from the use of any information it contains.

Open Access Article. Published on 03 April 2026. Downloaded on 4/26/2026 11:14:24 PM.  
This article is licensed under a Creative Commons Attribution-NonCommercial 3.0 Unported Licence.



## Sustainability Spotlight Statement

The shift from fossil resources to renewable lignocellulosic biomass is essential for a sustainable circular economy. However, conventional high-pressure fractionation is energy-intensive and degrades valuable biomass components. This work introduces a low-pressure flow-through system that significantly lowers energy barriers. It enables highly selective recovery of cellulose, thereby increasing enzymatic hydrolysis efficiency. Additionally, it extracts highly reactive lignin with well-preserved  $\beta$ -O-4 linkages, ensuring its viability for downstream chemical upgrades. We also implemented a strategy to reduce solvent use based on the reactor temperature profile, further enhancing the process. By minimizing resource consumption and maximizing the recovery of functional biopolymers, this approach supports the UN goals for responsible consumption and production (UN SDG 12).



## ARTICLE

**Low-pressure flow-through fractionation of *Quercus mongolica* for highly selective cellulose and reactive lignin recovery: a lignocellulosic biorefinery approach†**Imam Hidayat Nurwahid,<sup>a,b</sup> Sarah Keiza Ismail,<sup>a,b</sup> Vanny Natasya,<sup>a,b</sup> Jae-Wook Choi,<sup>a</sup> Kyeongsu Kim,<sup>a,b</sup> Seongmin Jin,<sup>a,b</sup> Hyunjoo Lee,<sup>a,b</sup> Chun-Jae Yoo,<sup>a,b,c,d</sup> Jeong-Myeong Ha,<sup>a,b</sup> and Chang Soo Kim<sup>\*a,b</sup>Received 00th January 20xx,  
Accepted 00th January 20xx

DOI: 10.1039/x0xx00000x

The utilization of lignocellulosic biomass (LCB) is the subject of intensive research and development due to the growing demand for sustainable, non-food-competitive alternatives to fossil fuels. Flow-through fractionation systems have shown potential for fully utilizing LCB, but the high-pressure requirements hinder their industrial implementation. This study investigated a low-pressure flow-through fractionation system for *Quercus mongolica*, designed for continuous-scale biorefinery operations. Results showed a 48.8% fractionation yield and 87.9% delignification, with a significant increase in enzymatic hydrolysis efficiency. Notably, the fractionated lignin exhibited substantially greater preservation of  $\beta$ -O-4 linkages than commercial Kraft lignin. A strategy to reduce solvent use was proposed based on the reactor temperature profile to further optimize the process. These results confirm the viability of this system as a lignocellulosic biorefinery pretreatment, enabling selective lignin separation and providing a scalable, continuous pathway for the complete valorization of LCB.

**Introduction**

The availability of lignocellulosic biomass, the most abundant renewable carbon source on Earth, has not been matched by its utilization, which has reached only 4.5% across various applications.<sup>1</sup> These underutilized resources, including agricultural waste (e.g., straw, bagasse), forestry residues (e.g., wood chips, sawdust), and the organic fraction of municipal solid waste, offer significant opportunities to convert them into a diverse range of bioproducts.<sup>2</sup> Lignocellulosic biorefineries have gained significant attention for their potential to improve energy security and address environmental issues, as well as for their ability to produce fuels and value-added products.<sup>3</sup> Full utilization of all biomass components is key to realizing this concept. However, lignin valorization remains a major bottleneck due to its chemical recalcitrance and structural complexity.<sup>4</sup> Therefore, the development of effective and efficient fractionation methods for lignocellulosic biomass requires careful consideration.

Regarding the economic feasibility of a lignocellulosic biorefinery, the utilization of lignin is recognized as paramount.

Therefore, researchers have developed a “lignin-first” approach that prioritizes lignin utilization from the design phase, enabling more complete utilization of lignocellulose.<sup>5</sup> The complex structure of native lignin contains multiple recurring linkages, the most prevalent being the  $\beta$ -aryl ether ( $\beta$ -O-4) motif. However, conventional fractionation methods primarily focus on pulping cellulose and pretreating sugars, typically under harsh conditions. This leads to lignin damage as a side effect, resulting in low-value products due to the condensation of the  $\beta$ -O-4 linkage motif. Therefore, developing a scalable strategy to extract native-like lignin with highly preserved  $\beta$ -O-4 linkages is crucial, especially for supplying advanced depolymerization processes.<sup>6</sup>

Numerous fractionation procedures have been developed to selectively extract lignin from lignocellulosic biomass, with organosolv processes being the most common.<sup>7,8</sup> Organosolv delignification uses an organic solvent (ethanol, acetone, and acetic acid), often with an acid co-catalyst and/or water, to break down the biomass structure.<sup>5,9,10</sup> Ethanol (EtOH) is a notably promising solvent due to its low cost, low toxicity, facile recovery via its low boiling point, and its ability to produce high-quality lignin byproducts.<sup>11,12</sup> A decisive advantage of this process is the excellent retention of the native  $\beta$ -O-4 linkages in extracted lignin. However, under acidic conditions, ethanol can also react with lignin through  $\alpha$ -alkoxylation to form a modified  $\beta'$ -O-4 motif, thereby retaining overall reactivity.<sup>13</sup> Ethanol-based organosolv has been widely applied to all primary lignocellulosic biomass types (hardwoods, softwoods, herbaceous crops, and agricultural wastes).<sup>11,14–16</sup> Despite producing relatively clean lignin suitable for value-added material production, the industrial application of this method

<sup>a</sup> Clean Energy Research Center, Korea Institute of Science and Technology (KIST), Seoul 02792, Republic of Korea.

<sup>b</sup> Division of Energy & Environment Technology, KIST School, University of Science and Technology (UST), Seoul 02792, Republic of Korea.

<sup>c</sup> School of Chemical Engineering, Sungkyunkwan University, Suwon 16419, Republic of Korea.

<sup>d</sup> KIST-SKKU Carbon-Neutral Research Center, Sungkyunkwan University, Suwon 16419, Republic of Korea.

†Electronic supplementary information (ESI) available. See DOI: 10.1039/x0xx00000x



remains limited by challenges such as the high temperatures and pressures required, as well as the often limited fractionation rate.<sup>17</sup> The system configuration is closely related to these limitations, as the fractionation methodology determines the degree of preservation of the lignin structure.

Batch fractionation methodologies are hindered by severe operating conditions, mainly high pressures (5–12 MPa) and the use of corrosive acid catalysts. These conditions pose significant challenges for industrial-scale-up and degrade lignin quality due to undesirable lignin condensation.<sup>18</sup> Recent advancements in flow-through systems have emerged as a promising alternative, as their short residence times and rapid temperature changes minimize carbohydrate and lignin degradation.<sup>19</sup> Flow reactors with high surface-to-volume ratios enable enhanced heat transfer, accelerating delignification and facilitating rapid separation of dissolved lignin. Precise control over these reaction times effectively preserves native aryl ether bonds and reduces condensation.<sup>4</sup> This is further confirmed by a comparative study that found that a semi-continuous process yields lignin with higher  $\beta$ -O-4 content and fewer condensed units than a batch system under identical conditions.<sup>20</sup> However, despite these advantages, designing a continuous system presents engineering challenges related to the presence of flammable solvents in a pressurized environment, which accelerates wear on seals and moving parts. Therefore, system durability can be improved by operating at lower pressures and avoiding the use of acid catalysts.

The potential of low-pressure flow-through fractionation as a scalable process for maximizing lignocellulosic biomass utilization warrants further study. Therefore, this study investigates the effects of operational parameters: temperature, pressure, solvent concentration, and reaction time. The forestry sector offers a sustainable alternative to fossil resources without disrupting global food security.<sup>21</sup> Therefore, the Mongolian oak (hardwood, *Quercus mongolica*), which covers 11% of forests in the Republic of Korea, is used as the lignocellulosic feedstock.<sup>22</sup> To determine the effectiveness of the pretreatment, the enzymatic digestibility of the fractionated biomass was evaluated. The experimental results in this study are expected to provide information on continuous, scale-up flow-through operation that can selectively separate components and preserve reactive lignin in a low-pressure system, thereby serving as a biorefinery pretreatment process.

## Experimental

### Materials

Mongolian oak (hardwood, *Quercus mongolica*) was provided by the National Institute of Forest Science, Republic of Korea, in small pieces and sieved to obtain a uniform size range (0.6–1.18 mm) for this study. Ethanol ( $\geq 99.6\%$ ), sulfuric acid (72 wt%), and a standard solution of sodium hydroxide (5N) were purchased from Daejung Chemicals and Metals Co., Ltd. (Siheung, Republic of Korea). Deuterated dimethyl sulfoxide (DMSO-d<sub>6</sub>, 99.9 atom% D) was purchased from Sigma-Aldrich (St. Louis,

Missouri, USA). Cellic® CTec2 Enzyme was purchased from Novozymes (Bagsværd, Denmark). Milled wood lignin (MWL) was extracted following the Björkman procedure.<sup>23</sup> Kraft lignin (KL) was purchased from West Fraser Ltd. (Hinton, AB, Canada).

### Low-pressure flow-through fractionation

The custom-built low-pressure flow-through fractionation reactor (1005 cm<sup>3</sup>) (Fig. S1) was loaded with 200  $\pm$  0.1 g of biomass sawdust. This biomass operated as a stationary packed bed. Fresh preheated solvent was continuously fed to the biomass-packed bed from a separate solvent tank at a constant rate of 30 mL/min. At the same time, the system was gradually heated to the target temperature. The pressure within the system increases with increasing temperature and reaction time. Since a specific pressure is required for this process, a relief valve maintains consistent system pressure, helping reduce the risk of clogging in the back-pressure regulator. Upon reaching the target pressure, the extract continues to flow through the bottom filter into a collection chamber. After the specified reaction time, the collected extract was processed. Distillation was performed to separate the extract into distinct outlet streams. These streams include the recovered ethanol for potential reuse and the concentrated liquid product, which contains the lignin-rich fraction. The solid pulp residue remaining in the biomass reactor represents the cellulose-rich fraction. This solid residue was collected and then oven-dried at 80 °C overnight. After drying, it was sieved into three particle-size fractions using a vibratory sieve shaker (AS 200 Control, RETSCH GmbH, Haan, Germany) for 15 minutes, with standard testing sieves for 0–0.325 mm, 0.325–0.6 mm, and 0.6–1.18 mm. Further analysis was performed on both products. In this study, the following operating conditions were varied: pressure (1–3 MPa at the relief valve), solvent concentration (0–100 vol% aqueous EtOH), temperature (18–190 °C), and reaction time (60 and 120 minutes).

### Compositional analysis

The carbohydrate and Klason lignin contents of biomass sawdust before and after the fractionation process (cellulose-rich fraction) were determined according to the Laboratory Analytical Procedure (LAP) of the National Renewable Energy Laboratory (NREL).<sup>24</sup> Hydrolyzed sugars were analyzed using high-performance liquid chromatography/HPLC (YL9100, YL Instruments, Republic of Korea) equipped with the Refractive Index Detector (RID). Isocratic separation was achieved at 60 °C on an Aminex HPX-87H column (300  $\times$  7.8 mm; Bio-Rad Laboratories, Inc., California, USA) using 5 mM H<sub>2</sub>SO<sub>4</sub> as the mobile phase at a flow rate of 0.6 mL/min.<sup>25</sup> Each analysis was performed three times. The concentrations of polymeric sugars (glucan and xylan) were determined from the corresponding monomer concentrations.<sup>26</sup> Following this, the concentrations of cellulose and hemicellulose were determined based on the glucose and xylose concentrations. Based on analytical results, the chemical composition of this hardwood species is 43.9% cellulose, 20.5% hemicellulose, 29.8% lignin, and 5.8% extractives. Delignification and cellulose/hemicellulose



retention percentages by mass (wt%) were calculated using the formulas presented below (1–3), as adapted from a previous publication.<sup>26</sup> Fractionation yields (wt%) were calculated using the equations presented in (4).

$$\text{Delignification (wt\%)} = \left(1 - \frac{\text{mass}_{\text{lignin in pulp sample}}}{\text{mass}_{\text{initial loaded lignin}}}\right) \times 100 \quad (1)$$

$$\text{Cellulose retention (wt\%)} = \left(1 - \frac{\text{mass}_{\text{glucan in pulp sample}}}{\text{mass}_{\text{initial loaded glucan}}}\right) \times 100 \quad (2)$$

$$\text{Hemicellulose retention (wt\%)} = \left(1 - \frac{\text{mass}_{\text{xylan in pulp sample}}}{\text{mass}_{\text{initial loaded xylan}}}\right) \times 100 \quad (3)$$

$$\text{Fractionation yield (wt\%)} = \left(\frac{\text{mass}_{\text{initial loaded pulp}} - \text{mass}_{\text{pulp after fractionation}}}{\text{mass}_{\text{initial loaded pulp}}}\right) \times 100 \quad (4)$$

### Biomass morphological analysis

The morphology of sawdust samples, both before and after fractionation (cellulose-rich fraction), was analyzed to assess the effect of different fractionation treatments on the surface morphology of the biomass. The analysis was conducted using the FEI Inspect™ F Field Emission Scanning Electron Microscope (FE-SEM) (Thermo Fisher Scientific Inc., USA).

### Enzymatic hydrolysis

The solid fraction was hydrolyzed to evaluate enzymatic digestibility. The distilled liquid was treated to assess its digestibility and to eliminate residual carbohydrates, yielding a purified lignin-rich fraction for structural analysis. For the solid-fraction hydrolysis, 1 g of unpretreated sawdust and the cellulose-rich fraction were each mixed with 30 mL of distilled water. For the liquid lignin-rich fraction, a 5N sodium hydroxide solution was added until the pH reached 5. Subsequently, Cellic® CTec2 enzyme (Novozyme, Denmark) was added to all samples at a loading of 20 filter paper units (FPU) per gram.<sup>27</sup> Each sample was transferred to a centrifuge tube and incubated for 72 hours at 50 °C with agitation at 20 rpm using a rotary shaker (Incubator Genie, Scientific Industries, Inc., USA).<sup>4</sup> Following the reaction, the supernatant was separated from the sediment by centrifugation (Heraeus Megafuge 8 Centrifuge, Thermo Scientific™, USA) at 4500 rpm for 5 min. The supernatants from all samples were then analyzed for fermentable sugar concentrations using HPLC (YL9100, YL Instruments, Republic of Korea) with a RID detector. Additionally, sediment from the enzymatically treated liquid fraction was collected and dried to yield purified lignin for structural analysis.

### Lignin structure analysis

The lignin product was dissolved in DMSO-d<sub>6</sub> at 10% (w/v). After complete dissolution, the solution was filtered and transferred to a 5 mm NMR tube. The two-dimensional (2D) <sup>1</sup>H-<sup>13</sup>C heteronuclear single-quantum coherence (HSQC) NMR spectra of lignin samples were acquired on a Bruker Ascend™

600 MHz spectrometer (Massachusetts, USA). Contour volume integration in the HSQC spectrum was used to calculate semi-quantitatively the relative abundance of lignin interunit linkages and monomer composition, with the C–H correlation signals of G2 (guaiacyl) and/or S2,6 (syringyl) used as references,<sup>28–30</sup> using the MestReNova software package (v14.3.3-33362, Mestrelab Research S.L., Spain). The center of the DMSO solvent peak was used as an internal reference ( $\delta_c/\delta_H$ : 40.19/2.50 ppm).

## Results and discussion

### Fractionation process conditions

The fractionation system has been designed to operate at pressures of up to approximately 3.5 MPa and to utilize a neutral solvent without a catalyst, facilitating scale-up. A parametric analysis of the effects of operating conditions, including pressure, temperature, and solvent concentration, on the organosolv fractionation of Mongolian oak has been conducted.

**Pressure.** According to experimental data obtained with 50 vol% ethanol, an internal reactor pressure of 1.1 MPa was achieved with the relief valve set to 1 MPa. Similarly, the 2 MPa and 3 MPa settings corresponded to internal pressures of 2.3 MPa and 3.4 MPa, respectively, due to the system flow rate. As shown in Fig. 1(a), the fractionation yield increases with system pressure. Fractionation yields are 26.9%, 48.8%, and 51.4% at 1.1 MPa, 2.3 MPa, and 3.4 MPa, respectively. The higher fractionation yield at higher pressure results from the increased cleavage of the bonding in the lignin-carbohydrate complexes (LCC) by the accelerated diffusion of the solvent into the LCC, as well as subsequent increased solubility of the cleaved fraction in the solvent due to a higher liquid-to-solid ratio in the reactor at higher pressure. This phenomenon has implications for delignification and hemicellulose retention. As depicted in Fig. 1(a), the delignification percentage increased with higher pressure applied (63.0%, 87.9%, and 95.4% at 1.1 MPa, 2.3 MPa, and 3.4 MPa, respectively). In comparison, hemicellulose retention decreased (49.0% at 1.1 MPa, 21.6% at 2.3 MPa, and 12.9% at 3.4 MPa). Therefore, this process enables effective dissolution of hemicellulose and lignin by water and ethanol in a flow-through system. On the other hand, cellulose retention was not significantly affected (approximately 89–92%).

**Solvent.** The importance of the cosolvent is illustrated in Fig. 1(b). Fractionation with water as the sole solvent resulted in the highest fractionation yield (56.7%), while mixed solvents of water and ethanol showed comparable fractionation yields (46.7–49.8%). This phenomenon is primarily attributed to the ability of water to disintegrate hemicellulose and induce swelling in cellulose structures (especially within amorphous regions). The loss of hemicellulose, a significant component that interacts with cellulose and lignin to strengthen cell walls,



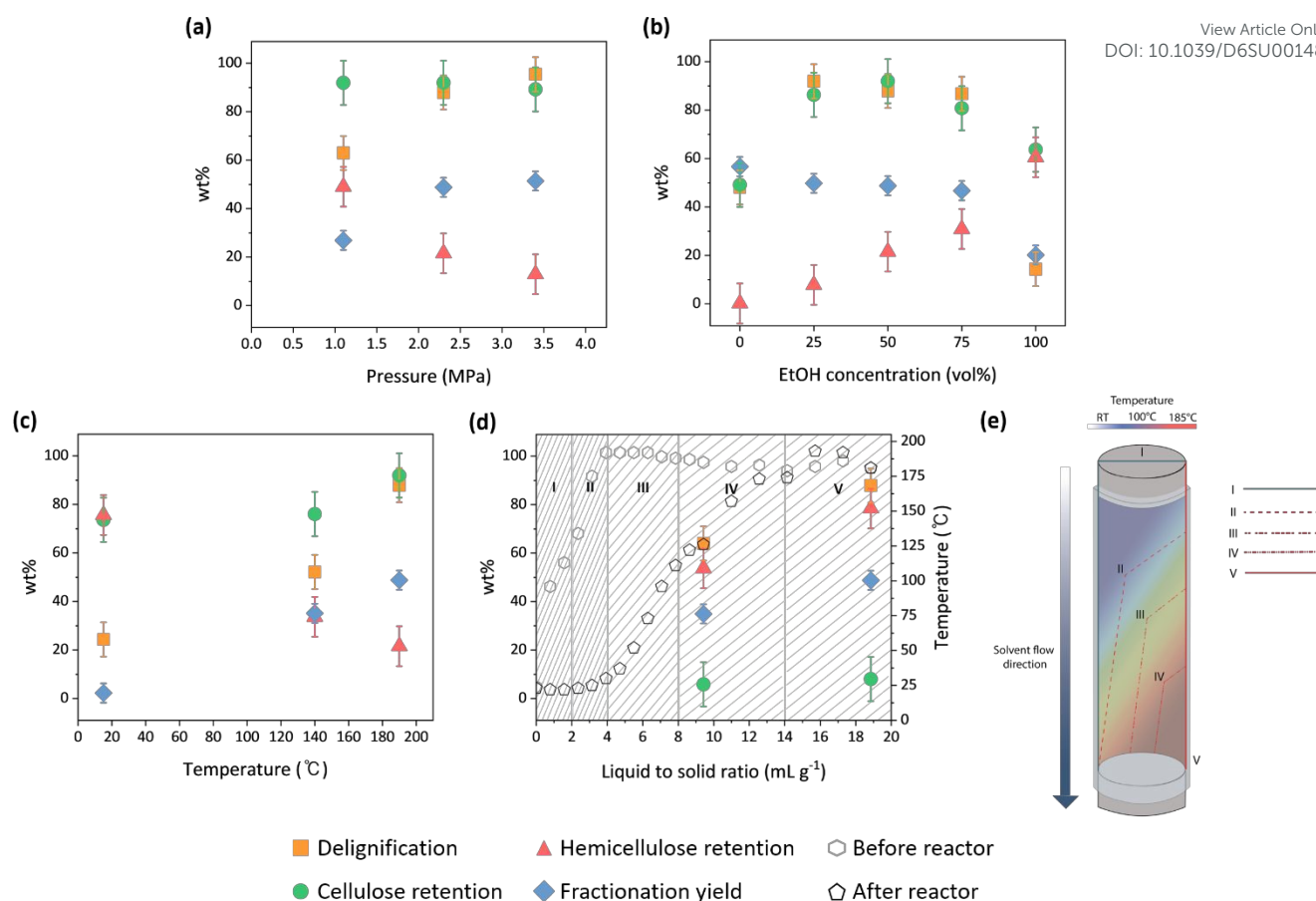


**Fig. 1** Organosolv fractionation of Mongolian oak as a function of (a) pressure (1.1 MPa, 2.3 MPa, and 3.4 MPa, with 50 vol% EtOH, at 190 °C for 120 min), (b) solvent concentration (0, 25, 50, 75, and 100 vol% EtOH, at 2.3 MPa, 190 °C for 120 min), (c) temperature (18 °C, 140 °C, and 190 °C with 50 vol% EtOH, at 2.3 MPa for 120 min), and (d) reaction time (expressed as liquid to solid ratio; 60 and 120 min, with 50 vol% EtOH, at 2.3 MPa, 190 °C); (e) Estimated temperature profiles at specific time duration inside the reactor.

increases solvent accessibility to cellulose and lignin.<sup>31–33</sup> Conversely, ethanol as the sole solvent yielded only 20.2%.

The use of water and ethanol as nucleophilic solvents is pivotal for promoting lignin cleavage and dissolving lignin fragments.<sup>34</sup> This mixed solvent therefore achieves higher delignification yields (86.7%–91.9%) than ethanol or water alone (14.3% and 48.1%, respectively). As with ethanol, the lack of synergism among nucleophilic agents results in less extensive delignification.<sup>35</sup> On the other hand, using water as a solvent can reduce delignification during fractionation because lignin is poorly soluble in water.<sup>36</sup>

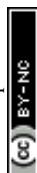
As the water-to-biomass ratio increases during autohydrolysis, hemicellulose retention declines significantly. This is attributed to the greater solubility of hemicellulose in water under these conditions.<sup>4,26</sup> The low cellulose retention of only 49% observed in water-only fractionation further exacerbates this issue. In contrast, cellulose retention remained high (80–92%) during fractionation with a mixed ethanol/water solvent, indicating that this mixture is a preferred approach for selective fractionation.

**Temperature.** The influence of temperature on organosolv fractionation of Mongolian oak has been investigated at 18 °C (room temperature), 140 °C, and 190 °C (basis condition) (Fig.

1(c)). Reduced fractionation yields were observed at lower temperatures, with specific values of 2.2% at room temperature, 35.1% at 140 °C, and 48.8% at 190 °C. The increased temperature can facilitate water ionization, improving the concentration of hydrogen ions and further enhancing the dissolution of hemicellulose.<sup>4</sup> This phenomenon is corroborated by experimental data showing a decrease in hemicellulose retention from 75.7% at room temperature to 21.6% at 190 °C.

**Reaction time.** Correlating the fractionation results with the temperature profile inside the reactor provides a meaningful interpretation of the time-dependent fractionation yield, solvent retention time, and the behavior of the fractionate in the reactor. This internal temperature profile is estimated from the temperatures measured immediately before and after the reactor at various processing durations. Because the solvent is continuously pumped into a fixed amount of biomass, the process duration directly determines the cumulative liquid-to-solid (L/S) ratio. This volumetric relationship over time is illustrated (Fig. 1(d)).

As the hot solvent progresses through the packed bed, the internal temperature profile evolves through five consecutive stages (Fig. 1(e)). Initially, the preheated solvent enters the



system and rapidly cools upon contacting the cold biomass (pattern I). Subsequently, the continuous supply of hot solvent, combined with conductive heating from the reactor walls, gradually raises the bulk biomass temperature (pattern II). The hydrodynamic residence time of the solvent in the reactor is approximately 25 minutes, which corresponds to an L/S ratio of 3.9. At this point, the first extract collection begins. However, the temperature immediately downstream of the reactor remains low at approximately 30 °C. This indicates that high-temperature fractionation is initially confined to a small portion of the upper biomass bed.

The thermal front progresses much more slowly than the flow of the physical solvent due to the heat capacity of the solid biomass and the gradual heat transfer into the flowing solvent. Complete bed heating and maximum fractionation occur when the high-temperature thermal front reaches the reactor outlet. This saturation happens around 85 minutes into the experiment, marking the start of pattern V. Although our experimental samples were collected up to a cumulative L/S ratio of 19 mL/g at 120 minutes, the temperature profile analysis reveals that an L/S ratio of 14 mL/g at 85 minutes is sufficient to achieve the maximum fractionation yield. This thermal mapping provides a direct strategy to optimize the process. By aligning extraction time with temperature progression, solvent use can be greatly reduced while still achieving effective fractionation.

Based on observations from the first hour of fractionation, delignification reached 64.0%, with cellulose and hemicellulose removal at 5.8% and 53.7%, respectively, and a fractionation yield of 34.93%. These numbers represent approximately 70% of the values obtained from the basis condition of two-hour fractionation, specifically delignification (87.9%), cellulose removal (8.0%), hemicellulose removal (78.4%), and fractionation yield (48.8%). The observation implies that a one-hour fractionation period corresponds to the temperature pattern IV in the reactor.

### Solid fraction characterization

**Particle size changes.** The change in the size distribution of biomass particles with pretreatment time was investigated by quantifying the mass of particles that passed through sieves of different mesh sizes.<sup>37</sup> The change in biomass particle size from an initial 0.6–1.18 mm is clearly correlated with applied pressure during fractionation (Fig. S2(a)). Particle size reduction due to fractionation was quantified as the ratio of particles smaller than their original size to those whose size remained unchanged. Particle size changes became more pronounced with increasing pressure (17.5% at 1.1 MPa, 27.1% at 2.3 MPa, and 35.2% at 3.4 MPa). This trend indicates that higher pressure facilitates bond cleavage between biomass components, thereby reducing particle size. The diffusion process begins at the exterior of the biomass sawdust, penetrates toward its core, disrupts intercomponent bonds, and dissolves hemicellulose and lignin.

The low particle-size reduction with increasing ethanol concentration (Fig. S2(b)) further indicates that ethanol can

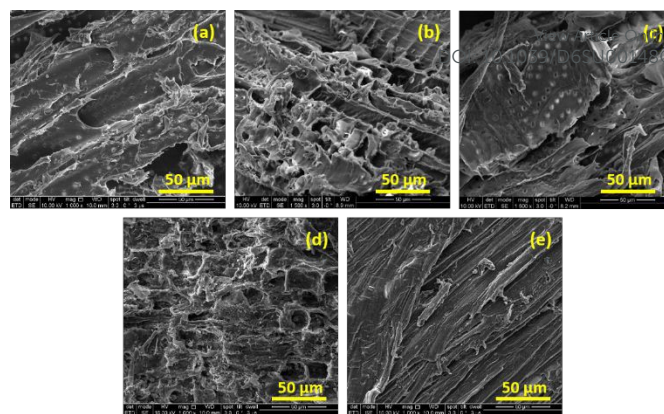


**Fig. 2** SEM images of (a) untreated Mongolian oak, after fractionation with 50 vol% EtOH at (b) 2.3 MPa and (c) 3.4 MPa under 1500 $\times$  magnifications, and after fractionation with (d) water and (e) 100 vol% EtOH under 1000 $\times$  magnifications.

disrupt van der Waals forces that hold lignin molecules together.<sup>38</sup> However, its efficacy is not comparable to the presence of water as a cosolvent. This means that the absence of water significantly reduced the extent of particle-size reduction during fractionation. In experiments conducted at different temperatures, the proportion of smaller particles increases as temperature rises, because higher temperatures significantly accelerate the reaction rate. For instance, the change in particle size increases dramatically from 4.6% at room temperature to 27.1% at 190 °C (Fig. S2(c)), which means harsher experimental conditions enhance particle size reduction. Furthermore, the percentage of smaller particles increases with longer fractionation times (Fig. S2(d)), consistent with the progressive nature of the process. These findings collectively highlight the distinct roles of ethanol and water: ethanol primarily facilitates dissolution of fractions, whereas water is essential for breaking intermolecular bonds among biomass components.

**Morphological changes.** The morphology of the samples, both before and after fractionation, was examined by SEM, which revealed a linear, fibrous structure of cellulose. The untreated sample had a relatively neat sheet arrangement with small holes (Fig. 2(a)). The sample after fractionation with an ethanol/water mixture (Fig. 2(b)) showed the formation of large holes and the exposure of cellulose fibers. This confirmed that a delignification process had occurred, releasing lignin from the cell walls.<sup>39</sup> Higher pressures during fractionation led to varying levels of structural degradation in the biomass (Fig. 2(c)). The results of fractionation with water (Fig. 2(d)) showed an irregular and rough appearance, indicating that the fibrous cellulose structure was affected by this process. Meanwhile, ethanol fractionation exhibited slight morphological changes (Fig. 2(e)).

**Illustration of the fractionation effect on biomass structure.** The biomass structure illustration was designed using analytical data on changes from the initial to the post-fractionation state to visualize the impact of fractionation. The main components of plant cell walls, cellulose, hemicellulose, and lignin, are



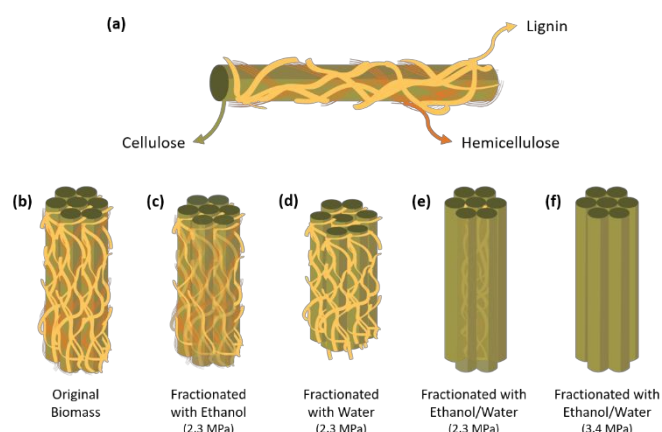


Fig. 3 Visual illustration of (a) the three main components of the plant cell wall, (b) original biomass before fractionation, and the impact of various fractionation conditions: (c) ethanol, (d) water, (e) ethanol/water, and (f) ethanol/water under higher pressure.

illustrated to mark the transformations that occur (Fig. 3(a)). Cellulose, the most abundant component, forms the structural framework by assembling long polymer chains into microfibrils that provide tensile strength. Hemicellulose, a heterogeneous group of polysaccharides, interacts extensively with cellulose microfibrils and is tightly bound within the cell wall, forming bonds that are crucial for organizing the microfibril network. Lignin, a highly cross-linked amorphous aromatic polymer, acts as an adhesive. It binds cellulose and hemicellulose, offering structural rigidity, stress protection, and hydrophobicity.<sup>2</sup>

The illustration of the original biomass (Fig. 3(b)) depicts the complex architecture of intact lignocellulosic material, with cellulose fibers tightly packed and interwoven with a hemicellulose-lignin matrix. This recalcitrant structure is the primary barrier to biocatalyst access to cellulose, affecting the enzymatic conversion efficiency. Fractionation with ethanol, although capable of promoting lignin solubilization, has shown limited effectiveness in completely separating lignin and hemicellulose (Fig. 3(c)). This is reflected in the high retention of lignin and hemicellulose relative to their initial weights (85.6 wt% and 62.0 wt%, respectively). Meanwhile, as illustrated in Fig. 3(d), water-only fractionation has caused significant cellulose damage (49.2 wt% retention). Despite successfully dissolving all hemicellulose, lignin retention remained high (52.0 wt%), indicating that lignin remained attached to the remaining cellulose structure. Ethanol/water fractionation yielded a more selective fraction than the sole-solvent process at the same pressure (Fig. 3(e)). The synergistic effects of the mixture resulted in significant removal of lignin and hemicellulose (12.1 wt% and 18.1 wt% retention, respectively), thereby increasing cellulose fiber exposure (92.0 wt% retention). Subsequently, fractionation at higher pressure (Fig. 3(f)) yielded a more effective separation, achieving the highest lignin and hemicellulose removal (4.6 wt% and 12.9 wt% retention, respectively) and producing highly purified cellulose fibers (89.2 wt% retention). The data and illustrations collectively demonstrate that fractionation can serve as a pretreatment to increase the accessibility of cellulose fibers,

thereby enhancing enzyme penetration and improving the efficiency of enzymatic hydrolysis. DOI: 10.1039/D6SU00148C

**Enzymatic accessibility of the solid fraction.** Enzymatic hydrolysis was performed to assess the applicability of this fractionation process as a biomass pretreatment method in a sugar-based biorefinery context. Enzymes require direct contact with cellulose for the hydrolysis process to occur.<sup>40</sup> However, the plant cell wall, particularly lignin, creates a barrier to the diffusion of cellulose-binding enzymes into the LCC and adhesion sites, thereby reducing their activity. The organosolv flow-through fractionation process in this study serves as a pretreatment that removes lignin and hemicellulose from the biomass after partial dismantling of the LCC, thus producing a cellulose-rich substrate. Cellulose-rich pulp from each fractionation process was treated with the CTec2 enzyme to evaluate the enzymatic hydrolysis performance.

The efficiency of enzymatic hydrolysis is measured by the percentage of initial cellulose and hemicellulose converted into fermentable sugars. As shown in Fig. 4(a), the fractionation process significantly affected the efficiency of enzymatic hydrolysis. Untreated sawdust exhibited a hydrolysis efficiency of 10.7%. The efficiency value was positively correlated with the percentage of delignification and the structural changes of the fractionated biomass, which aligns with the SEM images. Delignification and pore formation increased enzyme accessibility to cellulose within the biomass structure.<sup>41</sup> For instance, water-only fractionation yielded 36.3%. The use of ethanol and water as a cosolvent increased the efficiency to 66.8%. Furthermore, applying higher pressure with the cosolvent resulted in an even higher efficiency of 74.9%.

However, fractionation using ethanol as the sole solvent reduced hydrolysis efficiency to 8.1%. This decline likely results from limited dismantling, since water primarily degrades the structure by attacking hemicellulose. As a result, lignin on the outer surface of the biomass dissolves into ethanol. This keeps the LCC intact and can even cause the surface to harden through heat during fractionation. Enzyme diffusion into the biomass can be restricted, and high lignin levels are known to hinder enzyme adsorption. These factors collectively result in the lowest hydrolysis efficiency among the solid, cellulose-rich fractions. The observed phenomenon corresponds to the visual representation of how fractionation affects the three main plant cell wall components (Fig. 3). The synergistic effect of ethanol and water as cosolvents enhances the cleavage of bonds within the LCC structure.

Other biomass pretreatment methods, such as steam explosion and acid catalysis, can achieve high cellulose hydrolysis yields of 75–92%.<sup>42</sup> These methods rely on steam and acid to dismantle the LCC and convert hemicellulose into water-soluble pentoses. However, a significant drawback of these methods is the irreversible condensation of lignin, which converts valuable  $\beta$ -O-4 linkages into recalcitrant C–C bonds. In contrast, this study aims to maintain lignin quality under mild conditions, hence facilitating the scale-up of the continuous system. Further enhancement of the enzymatic hydrolysis of cellulose-rich pulp can also be achieved by optimizing the



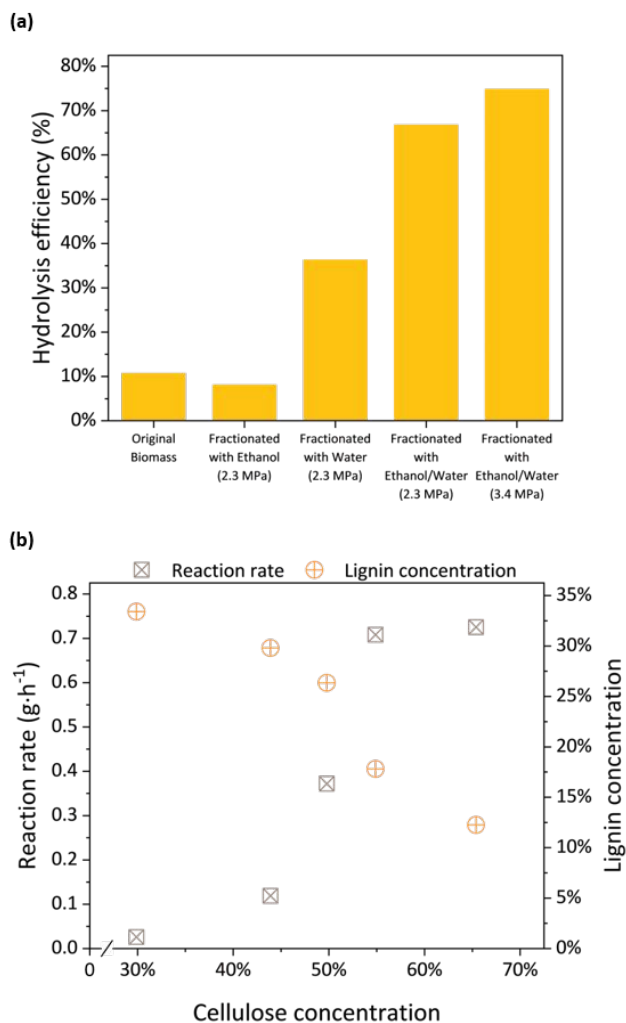


**Fig. 4** (a) Enzymatic hydrolysis efficiency and (b) cellulose reaction rate in the cellulose-rich fraction.

pretreatment process, which is critical for sugar-based biorefineries.

**Enzymatic hydrolysis rate of the solid fraction.** A well-known mechanism of enzymatic hydrolysis is that an increase in cellulose concentration corresponds to a greater surface area accessible to cellulase enzymes, leading to faster reaction kinetics. As shown in (Fig. 4(b)), the enzymatic hydrolysis reaction rate ( $\text{g}\cdot\text{h}^{-1}$ ) steadily increased as the cellulose concentration in the pretreated biomass rose. Simultaneously, the corresponding lignin concentration in these samples decreased. This clear inverse relationship confirms that delignification effectively dismantles the spatial barrier created by lignin, which would otherwise embed in the cellulose surface, limiting substrate swelling and preventing enzyme access to cellulose microfibrils. By removing this physical barrier and inhibitory component, the selective fractionation method (illustrated in Fig. 3) produces a highly purified, cellulose-rich fraction that can be more rapidly hydrolyzed into fermentable sugars, thereby validating its efficacy for biorefinery applications.

### Liquid fraction characterization

**Impact of fractionation conditions on lignin structure.** Lignin inter-unit linkages and subunits were semi-quantified from peak volume integration using the 2D  $^1\text{H}$ - $^{13}\text{C}$  HSQC NMR spectra (Fig. S3), with the results summarized in Table 1. In the aromatic regions, the NMR HSQC spectra of MWL and fractionated oak lignin display central aromatic units, primarily composed of syringyl (S) and guaiacyl (G) units. New signals at  $\delta_{\text{C}}/\delta_{\text{H}}$  81.9/4.76 were observed in the spectrum of the organosolv lignin fraction in the aliphatic side-chain regions. This signal was not found in the spectra of MWL, indicating the hydroxyl groups of  $\beta$ -O-4 linkages (A) were changed by the nucleophilic ethanol cosolvent and generated the methylene group in  $\alpha$ -ethoxylated  $\beta$ -O-4 linkages ( $\beta'$ -O-4, A').<sup>29,43</sup> The abundance of  $\beta'$ -O-4 ether bonds is directly proportional to the ethanol concentration of the solvent (Table 1).

**Table 1** Comparative quantitative analysis of lignin structural information (linking motifs per 100 C9 units) following flow-through fractionation of Mongolian oak under different conditions.

Samples	$\beta$ -O-4	$\beta'$ -O-4	S/G
MWL <sup>a</sup>	60.7	-	1.0
KL <sup>b</sup>	7.0	-	1.5
1.1 MPa	21.6	1.0	2.2
2.3 MPa	20.8	1.5	2.3
3.4 MPa	17.2	2.0	2.8
Water	10.8	-	1.8
25vol% EtOH	19.2	1.3	2.2
50vol% EtOH	20.8	1.5	2.3
75vol% EtOH	25.6	1.8	2.4
100vol% EtOH	27.2	1.9	2.4

<sup>a</sup>Milled wood lignin; <sup>b</sup>Kraft lignin

Quantitative analysis of primary lignin linkages (Table 1) was conducted using previously reported 2D-HSQC methods,<sup>29,30,44</sup> with results expressed per 100 aromatic units (100Ar) to enable internal standardization and accurate quantification of lignin structures. The content of  $\beta$ -O-4 linkages in the MWL was 60.7/100Ar, and it decreased to 21.6/100Ar, 20.8/100Ar, and 17.2/100Ar at 1.1 MPa, 2.3 MPa, and 3.4 MPa, respectively. The degradation of  $\beta$ -O-4 linkages at higher pressures suggests that the increased molecular density and associated higher heat content of the compressed solvent within the reactor drove this degradation during fractionation at the same temperature. The  $\beta$ -O-4 linkage content differed across solvents: 10.8/100Ar, 19.2/100Ar, 20.8/100Ar, 25.6/100Ar, and 27.2/100Ar in water, 25vol% EtOH, 50vol% EtOH, 75vol% EtOH, and 100vol% EtOH, respectively. These results indicate that increasing the ethanol-to-solvent ratio can increase the content of  $\beta$ -O-4 linkages in the lignin fraction. Water has a higher thermal energy content than



ethanol; upon transfer from the solvent to the substrate, it facilitates bond cleavage. Compared with technical lignin (e.g., Kraft lignin), the organosolv lignin produced in this study exhibited significantly higher quality due to three-times enrichment in  $\beta$ -O-4 linkages. This preserves the native reactivity of lignin, enhancing its value for downstream applications.

The difference in S/G ratio between MWL and fractionated lignin indicates a change in the relative proportions of S and G units, which are influenced by pressure and solvent during fractionation. The S/G ratio of fractionated lignin consistently exceeded that of MWL (1.0) under all tested conditions. Specifically, the ratio increased with increasing pressure (2.2 at 1.1 MPa, 2.3 at 2.3 MPa, and 2.8 at 3.4 MPa) and ethanol concentration (1.8 in water, 2.2 in 25 vol% EtOH, 2.3 in 50 vol% EtOH, 2.4 in 75 vol% EtOH, and 2.4 in 100 vol% EtOH). The observed difference in S/G ratio is primarily due to the greater susceptibility of G-type lignin to condensation reactions compared to S-type lignin.<sup>4,29,44,45</sup> This finding indicates an increased reactivity of G-type lignin to ethanol-mediated condensation.

**Enzymatic hydrolysis rate of the liquid fraction.** Based on the calculations (Fig. S4), the rate of hemicellulose enzymatic hydrolysis in the lignin-rich fraction generally increased with higher hemicellulose concentrations and was unaffected by lignin levels. However, a notable deviation was observed in the liquid product obtained from fractionation with ethanol as the sole solvent, as indicated by the red circles. Despite having the highest hemicellulose concentration, this sample exhibited a near-zero enzymatic reaction rate. This severe reduction in hydrolysis efficiency is not primarily driven by lignin concentration or process severity. Instead, it is attributed to the inhibitory effect of high ethanol concentration in this product. Commercial enzyme cocktails, such as CTec2, require an aqueous environment to maintain their active three-dimensional protein structures. The high concentration of residual organic solvent in the liquid fraction likely induced severe solvent denaturation and dehydration of the enzyme proteins.<sup>46–48</sup> Consequently, the enzymes were rapidly inactivated. This halted the hydrolysis process entirely, regardless of the abundant hemicellulose substrate available in the liquid.

### Prospects for lignocellulosic biorefinery

**Scale-up and continuous process.** Designing continuous fractionation systems to operate at the lowest possible pressure is a fundamental priority, as it directly reduces mechanical stress and potential energy within the system, the primary drivers of component fatigue and structural failure. This approach can extend system lifespan and decrease the risk of catastrophic failure, ultimately lowering maintenance costs. Operational safety is also enhanced, particularly when handling flammable solvents. Additionally, this approach broadens the range of material options available for system construction. However, a primary challenge lies in balancing the need for low

pressure with the requirements for effective fractionation and achieving the necessary phase separation.

Maintaining equipment integrity and the sustainability of the entire fractionation process are crucial, particularly through the selection of low-boiling-point neutral solvents. Recently, innovations such as Deep Eutectic Solvents (DESs) and Ionic Liquids (ILs) have gained popularity. However, these solvents are complex and require significant energy to recycle. Low-boiling solvents, by contrast, can be readily recycled through simple distillation, thereby reducing solvent consumption, lowering operational costs, and lessening environmental impact. Furthermore, managing flammable solvents is also a crucial safety consideration. Although ethanol is a low-boiling solvent, its flammability poses a risk. One way to minimize this risk is by mixing it with water. Selecting the optimal water-to-ethanol ratio is influential for maintaining high fractionation yields and lignin reactivity while mitigating these risks. This optimization also provides economic benefits by reducing the energy required for ethanol distillation during the recycling phase.

The importance of mild fractionation for potential sustainable biorefinery applications is highlighted in this study. Conducted at relatively low pressure (2.3 MPa) without acid catalysts, this flow-through organosolv process achieved 87.9% delignification. This result is highly competitive when compared to prior research (Table S1). Specifically, it surpasses the 79.0% delignification reported for the batch organosolv treatment of eucalyptus residues, which relied on a concentrated acid catalyst.<sup>11</sup> Additionally, this method exceeds the 84.9% delignification achieved in a high-pressure 19.0 MPa flow-through system utilizing *Pinus taeda*.<sup>35</sup> Furthermore, the organosolv process used in this work produced lignin of higher quality compared to standard technical lignins, such as Kraft lignin. This improved quality is demonstrated by significant preservation of structural integrity, as indicated by a total  $\beta$ -O-4 linkage content of 20.8/100Ar, compared to 7.0/100Ar (Table 1). This preservation is notably better than the 2.0/100Ar reported for acid-catalyzed batch processing of poplar.<sup>28</sup> Although a higher  $\beta$ -O-4 content of 43.0/100Ar was reported for the flow-through treatment of beech wood, that specific process operated at a much lower temperature of 120 °C, which compromised the overall delignification yield, reaching only 73.0%.<sup>6</sup> Therefore, this study approach offers an optimal balance of high delignification efficiency and lignin quality.

Additional optimization of solvent use can be achieved by adjusting the reactor temperature via heat transfer, as previously shown in the current setup and under the basis condition of 14 mL/g (12.5 g solvent per g biomass). Further solvent reduction for the same performance can be achieved by enhancing heat transfer in the reactor.

**Fractionates as intermediate products for lignocellulosic biorefinery.** The complex mass streams of the main hardwood components, starting from the original sawdust through the fractionation and hydrolysis stages, are visually traced in (Fig. 5). The high selectivity of the flow-through fractionation process is immediately evident. The vast majority of hemicellulose and



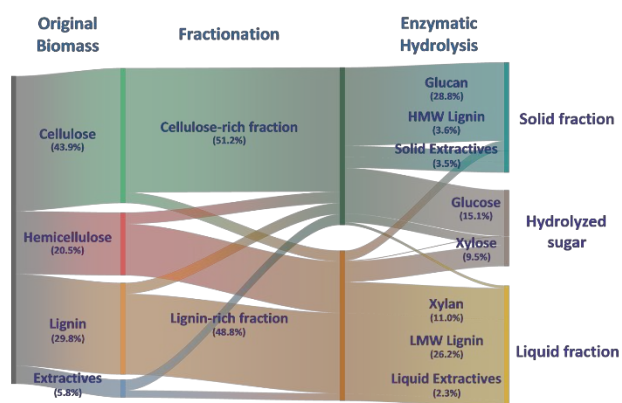


**Fig. 5.** Mass balance of organosolv fractionation at the basis condition (2.3 MPa, 50 vol% EtOH, 190 °C, 2 h) and the hydrolyzed sugar. HMW Lignin: High Molecular-Weight Lignin; LMW Lignin: Low Molecular-Weight Lignin.

lignin was separated into the liquid stream, which corresponds to the lignin-rich fraction. Conversely, the majority of cellulose remained as a stationary solid, representing the cellulose-rich pulp fraction. Following enzymatic hydrolysis, three main products were obtained: a solid fraction, a liquid fraction, and hydrolyzed sugar. The solid fraction contained glucan, a cellulose intermediate, as its main component, in addition to high-molecular-weight lignin and insoluble solid extractives. Meanwhile, the liquid fraction was predominantly composed of low-molecular-weight lignin, with xylan (a hemicellulose intermediate) and soluble extractives also present. The glucan and xylan listed in the final solid and liquid fractions are the unreacted polymer that remained unconverted after the hydrolysis step. The solid cellulose product can be used as a fiber or in other carbon-based applications, or hydrolyzed to produce fuels or chemicals.<sup>49</sup> Furthermore, the produced lignin exhibits high reactivity, further expanding its applicability in biorefinery processes. Subsequent valorization of these intermediates could be a focus of future work in lignocellulosic biorefineries, serving as an alternative to oil refineries.

## Conclusions

The effectiveness of a low-pressure flow-through fractionation system for extracting lignocellulose components from hardwood was successfully demonstrated in this study. The fractionation yield and selectivity were significantly influenced by key process parameters, especially pressure and solvent concentration. Notably, the ethanol/water cosolvent improved results compared to single-solvent systems. However, a trade-off existed between yield and lignin quality, which was considered when applying pressure to the system. The leading indicator of lignin quality, the preservation of  $\beta$ -O-4 linkages, was up to three times higher than in commercial Kraft lignin. Based on the reactor temperature profile, a 26.3% reduction in solvent consumption (to 5 mL/g of biomass) is proposed as a process improvement strategy. Particle-size distribution calculations and SEM images confirmed the physical changes resulting from fractionation, effectively exposing the cellulose.

Consequently, the enzymatic hydrolysis efficiency increased substantially, from 10.7% for untreated sawdust to 66.8% for the fractionated sample. These findings can inform the design of continuous, low-pressure biorefinery pretreatment systems that selectively separate biomass components and recover reactive lignin.

## Author contributions

Imam Hidayat Nurwahid: Methodology, Formal analysis, Investigation, Writing – Original draft. Sarah Keiza Ismail: Methodology. Vanny Natasya: Visualization. Jae-Wook Choi: Writing – review & editing. Kyeongsu Kim: Writing – review & editing. Seongmin Jin: Writing – review & editing. Hyunjoo Lee: Writing – review & editing. Chun-Jae Yoo: Writing – review & editing. Jeong-Myeong Ha: Writing – review & editing. Chang Soo Kim: Conceptualization, Writing – review & editing, Supervision, Funding acquisition.

## Conflicts of interest

There are no conflicts to declare.

## Data availability

The data supporting this article have been included as part of the ESI. Reference 50 is cited in the ESI.

## Acknowledgements

This work was supported by the Korea Institute of Science and Technology institutional program (2E33852, 2E33931) and the Ministry of Trade, Industry, and Energy green car program (RS-2024-00507722). The authors appreciate Dr. Hanseob Jeong of the Korea National Institute of Forest Science for providing Mongolian oak. The authors are grateful to the KIST Advanced Analysis Center (Seoul, Republic of Korea) for SEM and 2D-HSQC NMR analysis.

## References

- M. Mujtaba, L. Fernandes Fraceto, M. Fazeli, S. Mukherjee, S. M. Savassa, G. Araujo de Medeiros, A. do Espírito Santo Pereira, S. D. Mancini, J. Lipponen and F. Vilaplana, *J. Clean. Prod.*, 2023, **402**, 136815.
- M. H. Tanis, O. Wallberg, M. Galbe and B. Al-Rudainy, *Molecules*, 2023, **29**, 98.
- C. Lai, C. Yang, Y. Jia, X. Xu, K. Wang and Q. Yong, *Bioresour. Technol.*, 2022, **355**, 127255.
- H. Zhou, Q. Liu, X. Zhong, Y. Chu, Z. Wang and Y. Wang, *Ind. Crops Prod.*, 2021, **173**, 114124.
- M. M. Abu-Omar, K. Barta, G. T. Beckham, J. S. Luterbacher, J. Ralph, R. Rinaldi, Y. Román-Leshkov, J. S. M. Samec, B. F. Sels and F. Wang, *Energy Environ. Sci.*, 2021, **14**, 262–292.



- 6 D. S. Zijlstra, C. A. Analbers, J. de Korte, E. Wilbers and P. J. Deuss, *Polymers (Basel)*, 2019, **11**, 14–17.
- 7 T. Pang, G. Wang, H. Sun, W. Sui and C. Si, *Ind. Crops Prod.*, 2021, **165**, 113442.
- 8 X. Zhao, K. Cheng and D. Liu, *Appl. Microbiol. Biotechnol.*, 2009, **82**, 815–827.
- 9 A. Johansson, O. Aaltonen and P. Ylinen, *Biomass*, 1987, **13**, 45–65.
- 10 J. Wildschut, A. T. Smit, J. H. Reith and W. J. J. Huijgen, *Bioresour. Technol.*, 2013, **135**, 58–66.
- 11 F. Carvalheiro, L. C. Duarte, F. Pires, V. Van-Dúnem, L. Sanfins, L. B. Roseiro and F. Gírio, *Energies (Basel)*, 2022, **15**, 5654.
- 12 K. J. Yong and T. Y. Wu, *Bioresour. Technol.*, 2023, **384**, 129238.
- 13 D. S. Zijlstra, C. W. Lahive, C. A. Analbers, M. B. Figueirêdo, Z. Wang, C. S. Lancefield and P. J. Deuss, *ACS Sustain. Chem. Eng.*, 2020, **8**, 5119–5131.
- 14 W. J. J. Huijgen, A. T. Smit, J. H. Reith and H. Den Uil, *Journal of Chemical Technology and Biotechnology*, 2011, **86**, 1428–1438.
- 15 T. M. Santos, V. Rigual, J. C. Domínguez, M. V. Alonso, M. Oliet and F. Rodriguez, *Biomass Convers. Biorefin.*, 2024, **14**, 451–464.
- 16 S. Bauer, H. Sorek, V. D. Mitchell, A. B. Ibáñez and D. E. Wemmer, *J. Agric. Food Chem.*, 2012, **60**, 8203–8212.
- 17 J. Xu, C. Li, L. Dai, C. Xu, Y. Zhong, F. Yu and C. Si, *ChemSusChem*, 2020, **13**, 4284–4295.
- 18 J. Yao, M. Karlsson, M. Lawoko, K. Odellius and M. Hakkarainen, *RSC Sustainability*, 2023, **1**, 1211–1222.
- 19 J. Xu, Z. Shao, Y. Li, L. Dai, Z. Wang and C. Si, *Ind. Crops Prod.*, 2021, **164**, 113350.
- 20 A. T. Smit, M. Hoek, P. A. Bonouvrie, A. van Zomeren, L. A. Riddell and P. C. A. Bruijninx, *ACS Sustain. Chem. Eng.*, 2024, **12**, 4731–4742.
- 21 A. Zoghalmi and G. Paës, *Front. Chem.*, 2019, **7**, 874.
- 22 D. Kweon and P. G. Comeau, *For. Ecol. Manage.*, 2021, **502**, 119727.
- 23 A. Björkman, *Nature*, 1954, 1057–1058.
- 24 A. Sluiter, B. Hames, R. O. Ruiz, C. Scarlata, J. Sluiter, D. Templeton and D. Crocker, *Laboratory Analytical Procedure (LAP): Determination of Structural Carbohydrates and Lignin in Biomass*, Golden, Colorado, 2012.
- 25 D.-W. Kim, S. M. Kim, I. H. Nurwahid, C. S. Kim, J. Lee, S. W. Eun, C. Sung, G. Gong, J. K. Ko, Y. Um, S. O. Han and J. H. Ahn, *Bioresour. Technol.*, 2025, **435**, 132860.
- 26 J. H. Jang, A. R. C. Morais, M. Browning, D. G. Brandner, J. K. Kenny, L. M. Stanley, R. M. Happs, A. S. Kovvali, J. I. Cutler, Y. Román-Leshkov, J. R. Bielenberg and G. T. Beckham, *Green Chemistry*, 2023, **25**, 3660–3670.
- 27 J. K. Ko, Y. Um, H. M. Woo, K. H. Kim and S. M. Lee, *Bioresour. Technol.*, 2016, **209**, 290–296.
- 28 X. Meng, S. Bhagia, Y. Wang, Y. Zhou, Y. Pu, J. R. Dunlap, L. Shuai, A. J. Ragauskas and C. G. Yoo, *Ind. Crops Prod.*, 2020, **146**, 112144.
- 29 X. Wang, Y. Guo, J. Zhou and G. Sun, *RSC Adv.*, 2017, **7**, 8314–8322.
- 30 C. Zhao, J. Huang, L. Yang, F. Yue and F. Lu, *Ind. Eng. Chem. Res.*, 2019, **58**, 5707–5714.
- 31 T. H. Kim and Y. Y. Lee, *Bioresour. Technol.*, 2006, **97**, 224–232.
- 32 H. V. Scheller and P. Ulvskov, *Annu. Rev. Plant Biol.*, 2010, **61**, 263–289.
- 33 A. Etale, A. J. Onyianta, S. R. Turner and S. J. Eichhorn, *Chem. Rev.*, 2023, **123**, 2016–2048.
- 34 M. H. Hamzah, S. Bowra and P. Cox, *Processes*, 2020, **8**, 845.
- 35 D. Pasquini, M. T. B. Pimenta, L. H. Ferreira and A. A. D. S. Curvelo, *J. Supercrit. Fluids*, 2005, **36**, 31–39.
- 36 J. D. Sheehan, E. Ebikade, D. G. Vlachos and R. F. Lobo, *ACS Sustain. Chem. Eng.*, 2022, **10**, 11117–11129.
- 37 S. J. Kim, B. H. Um, D. J. Im, J. H. Lee and K. K. Oh, *Energies (Basel)*, 2018, **11**, 2457.
- 38 M. Broda, D. J. Yelle and K. Serwańska, *Molecules*, 2022, **27**, 8717.
- 39 Y. Han, Y. Bai, J. Zhang, D. Liu and X. Zhao, *Bioresour. Bioprocess.*, 2020, **7**, 24.
- 40 X. Meng, T. Wells, Q. Sun, F. Huang and A. Ragauskas, *Green Chemistry*, 2015, **17**, 4239–4246.
- 41 C. S. Lancefield, I. Panovic, P. J. Deuss, K. Barta and N. J. Westwood, *Green Chemistry*, 2017, **19**, 202–214.
- 42 Y. Yu, J. Wu, X. Ren, A. Lau, H. Rezaei, M. Takada, X. Bi and S. Sokhansanj, *Renewable and Sustainable Energy Reviews*, 2022, **154**, 111871.
- 43 Y. Guo, J. Zhou, J. Wen, G. Sun and Y. Sun, *Ind. Crops Prod.*, 2015, **76**, 522–529.
- 44 J. L. Wen, T. Q. Yuan, S. L. Sun, F. Xu and R. C. Sun, *Green Chemistry*, 2014, **16**, 181–190.
- 45 Y. Pu, S. Cao and A. J. Ragauskas, *Energy Environ. Sci.*, 2011, **4**, 3154–3166.
- 46 P. A. Skovgaard, B. H. Christensen, C. Felby and H. Jørgensen, *J. Ind. Microbiol. Biotechnol.*, 2014, **41**, 637–646.
- 47 M. Holtzapfel, M. Cognata, Y. Shu and C. Hendrickson, *Biotechnol. Bioeng.*, 1990, **36**, 275–287.
- 48 R. A. Sheldon and J. M. Woodley, *Chem. Rev.*, 2018, **118**, 801–838.
- 49 A. Smit and W. Huijgen, *Green Chemistry*, 2017, **19**, 5505–5514.
- 50 Y. Tobimatsu, F. Chen, J. Nakashima, L. L. Escamilla-Trevino, L. Jackson, R. A. Dixon and J. Ralph, *Plant Cell*, 2013, **25**, 2587–2600.



### Data availability

The data supporting this article have been included as part of the ESI. Reference 50 is cited in the ESI.

